Downstream Plasma Technology for Cleaning TEM Samples on Carbon Films

Lianfeng Fu,[1]* Haifeng Wang,[1] Christopher G. Morgan,[2] and Vincent Carlino[2]
[1]Western Digital Corporation, 44100 Osgood Road, Fremont, CA 94539
[2]IBSS Group Inc., 1559B Sloat Blvd., Suite 270, San Francisco, CA 94132
*Lianfeng.Fu@wdc.com

Introduction

With the advent of modern scanning/transmission electron microscopy (S/TEM) capable of higher resolution, better contrast, and faster throughput, it is imperative to ensure the cleanliness of the TEM sample under the ultrahigh vacuum conditions of the microscopes [1–5]. It is well known that sample contamination can severely deteriorate the quality of electron microscopy analysis of materials, especially as the sample regions of interest decrease in size. The adverse effects of sample contamination include obscuring the area of the sample being analyzed by buildup of a carbonaceous layer, interfering with focusing and astigmatism correction, and generating unexpected microanalysis signals [2, 3].

A variety of cleaning methods, including electron beam flooding, heating and/or cooling, ultraviolet light exposure, and plasma cleaning, have been developed to minimize sample contamination [4, 5]. Among them, plasma cleaning is considered the most effective way to prepare samples for electron microscopy. As shown in Figure 1a, a plasma can be described as an ionized gaseous state created by direct current (DC), radio frequency (RF), or microwave glow discharge, in which electrons, ions, and radicals coexist. The interaction of these plasma species with a solid surface causes three basic phenomena that lead to surface cleaning: heating from the electron-specimen interaction, sputtering from the ion-specimen interaction, and etching from the radical-specimen interaction [2]. Although the combination of all three plasma species is efficient in terms of cleaning rates, it can cause irreversible surface modification and undesirable heating. More problematically, as the plasma cleaning process removes the hydrocarbon contamination layer, it removes other carbon structures at the same time. This can be an issue for TEM carbon film users because the carbon film is extensively used as a support on TEM grids for both materials science and biological applications. For example, our laboratory routinely loads from 10 to 50 *ex-situ* lifted-out TEM samples on a carbon film Cu-grid in order to support the high volume wafer-based manufacturing process [6]. If the carbon support film is damaged before the hydrocarbon contamination layer on the TEM samples is removed, valuable information in TEM samples will be lost. Therefore, it is essential to develop a method that removes only the hydrocarbon contamination layer while preserving the carbon support film.

Downstream oxygen plasma is one technology that has been extensively used in modern semiconductor and

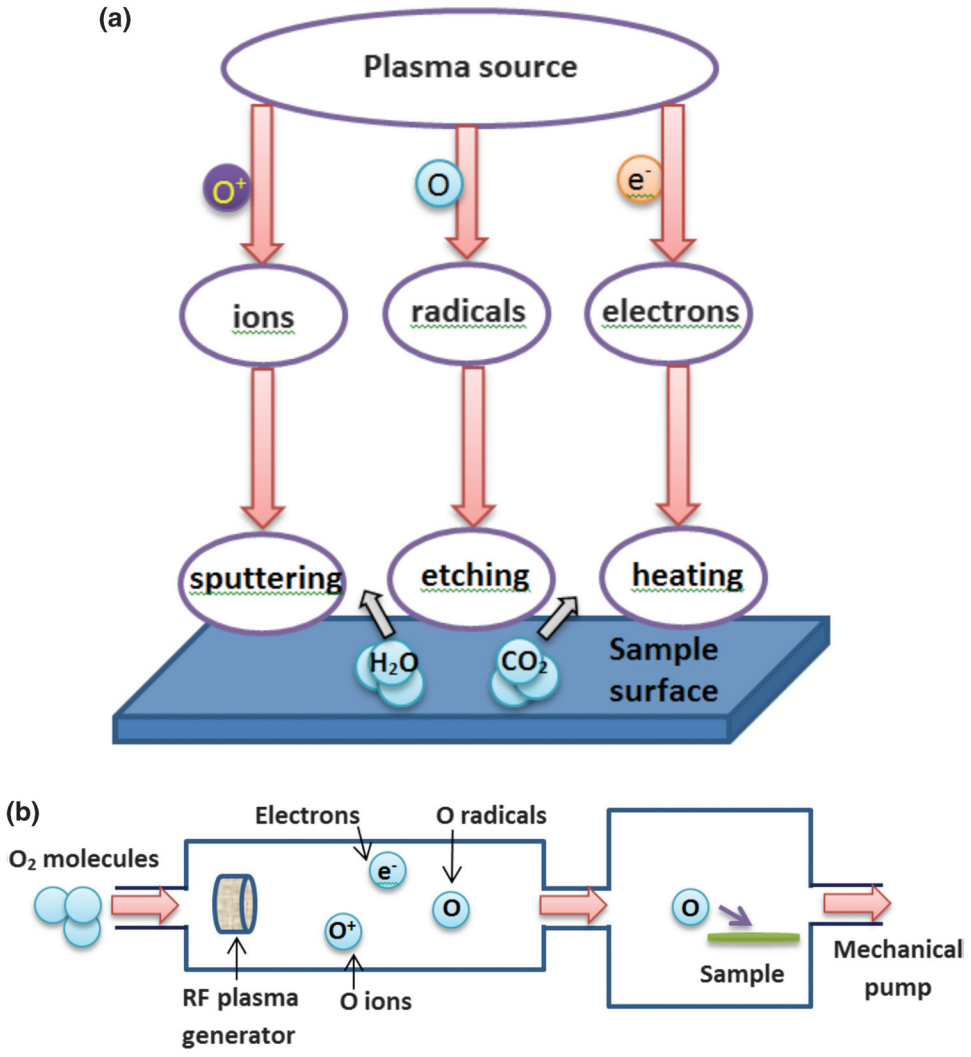

Figure 1: (a) Schematic representation of typical plasma cleaning mechanisms. (b) Schematic representation of a downstream plasma ashing system.

 doi:10.1017/S1551929513001260

microelectronic manufacturing production lines as a dry ashing process [7, 8]. In the downstream oxygen plasma ashing process, the samples are not directly immersed in the glow discharge. Instead, they are positioned downstream or remote from the plasma source as shown in the Figure 1b. This is in contrast to the traditional plasma ashing process where the samples are directly immersed in the glow discharge and could suffer kinetic reactions with the accelerated ions and electrons from the plasma source. With this downstream setup, the plasma species, including ions, electrons, and radicals, are energetically relaxed and recombined upon arrival at the remotely positioned samples. Thus, only a large number of non-energetic radicals can reach the vacuum chamber and react with the sample surfaces for ashing. Because of the nature of radicals, the ashing process is relatively gentle and does not produce kinetic bombardment, sputter damage, or sample heating, unlike the traditional plasma ashing process. Recently, IBSS Group Inc. has adopted this technology into the GV10x downstream plasma asher system for materials science and electron microscopy applications. This downstream plasma asher system can be used as an *in-situ* cleaner for scanning electron microscope (SEM) and focused ion beam (FIB) microscope chambers or can be customized into a portable system for TEM sample cleaning. In this work, we report the results of a systematic evaluation of the GV10x downstream plasma asher system in removing hydrocarbon contamination of TEM samples, primarily on holey carbon Cu-grids.

Materials and Methods

Figure 2a shows the layout of the GV10x DS plasma asher system in our laboratory. It is mainly composed of three components: plasma asher source, vacuum chamber, and RF controller. The plasma asher source is mounted to the vacuum chamber directly. In this way, no obstruction is introduced into the downstream flow of the source so that the highest cleaning efficiency can be achieved. The ashing gas can be room air or a mixture of Ar and O_2 gases. In our case, we use clean dry air (CDA) in order to avoid the impact of moisture variation. The GV10x asher source is fitted with a variable constriction valve to accommodate a large operating pressure range from 2.0 Torr to below 0.4 mTorr. The operating pressure depends on the speed of the vacuum pumps used to evacuate the chamber and the throughput of the vacuum valve. When the GV10x source is mounted on a turbo molecular-pumped SEM or dual-beam FIB chamber, the base chamber pressure can be < 0.4 mTorr. With a dry vacuum pump (scroll pump), the base pressure ranges between 50 mTorr and 500 mTorr. The vacuum chamber can be fitted with two different TEM holder ports simultaneously, for example, an FEI holder port and a JEOL holder port. The position of the port ensures that the sample for cleaning is immersed right at the center of the vacuum chamber and along the downstream flow direction of the source. Figure 2b shows the RF source control panel and its user interface. The operating parameter screen allows the user to set the operating parameters such as ignition plasma power, actual work power, and run time by using the

Figure 2: (a) Assembly of the GV10x downstream plasma Gentle Asher system showing the downstream plasma asher source, vacuum chamber, and two TEM holder ports. (b) GV10x controller panel showing the user interface and buttons.

up/down or increase/decrease buttons. Our laboratory uses the factory-recommended power at 50 watts, although the power can be adjusted to values between 10 and 99 watts.

TEM/STEM imaging, energy dispersive X-ray (EDX), and electron energy loss spectroscopy (EELS) analyses were carried out on a 200 kV Schottky field-emission gun (FEG) FEI Tecnai F20 ST microscope. This microscope is fully loaded with an analytical pole-piece objective lens, an EDAX X-ray detector, and a Tridiem Gatan image filter (GIF) spectrometer. The energy resolution for low-loss EELS spectra is typically 0.90 eV. Each EELS spectrum was corrected for dark current and spectrometer gain variations.

Results

Cleaning the carbon film itself. Before we evaluate the hydrocarbon contamination cleaning effect, it is worthwhile to study the impact of downstream plasma ashing on the holey carbon film alone. A primary reason is that tens of our TEM samples are loaded on the holey carbon film grid as mentioned earlier. We do not want to take the risk of losing TEM samples if the carbon film breaks while being cleaned. In order to find out the safe time window when the holey carbon film can still survive during downstream plasma ashing, we have applied a multi-step scheme in the design of the experiment.

In this scheme we first load the blank holey carbon film Cu grid in the microscope and take an image as reference. Then, we take out the grid, plasma ash it with a certain time, and reload it in the microscope. Thus, the downstream plasma ashing time we state is a cumulative time. Figures 3a to 3b show a series of images of holey carbon film supported Cu-grid with this multi-step scheme. As can be seen in the images, the contrast of the holey carbon film decreases with the increasing time. This indicates the thickness of holey carbon film may be decreasing with increasing downstream plasma ashing time. At the longest downstream plasma ashing time of 720 s, the holey carbon film barely shows contrast, and some film areas become ruptured. At this situation, we consider the holey carbon film unusable. We did a similar experiment with the traditional plasma cleaner, and the holey carbon film break-up time was less than 20 s. Thus, the downstream plasma ashing system shows an obvious improvement compared to the traditional one. This also supports the gentle ashing mechanism of radicals mentioned earlier.

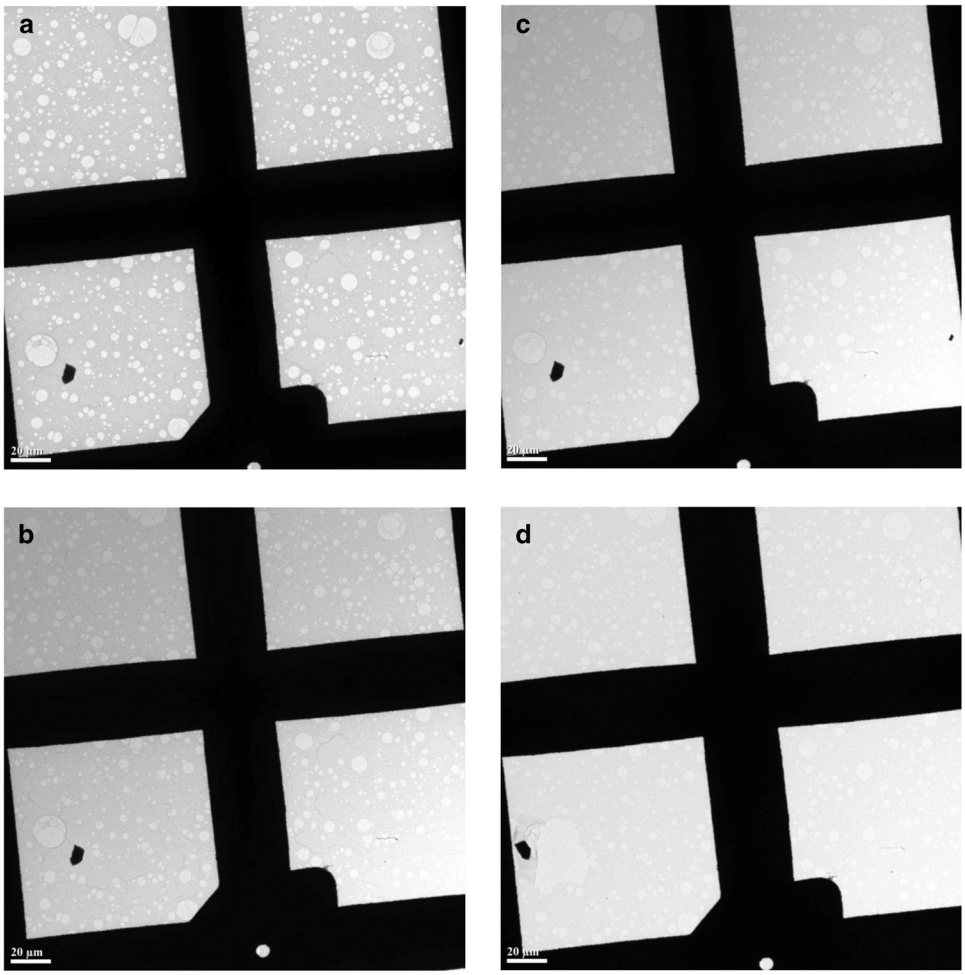

Figure 3: Images of holey carbon film supported Cu-grid before and after downstream plasma ashing: (a) 0s, (b) 240s, (c) 480s, (d) 720s.

Carbon film thickness changes. In order to validate the thickness change of holey carbon film during the downstream plasma ashing process, we used EELS analysis. It is well established that EELS can provide quick and reliable measurement of local thickness from both crystalline and amorphous samples. Sample thickness can be calculated by straightforward integration of the low-loss EELS spectrum with the following formula [9]:

$$t = \lambda \times \ln(I_T / I_0) \quad (1)$$

where t is the sample thickness, λ is the characteristic mean free path of inelastic scattering for the material, I_T is the total integrated intensity of electrons in the EELS spectrum, and I_0 is the intensity of electrons having lost no energy, namely the zero-loss peak (ZLP). Figure 4a shows the relative changes of the low-loss EELS spectra of holey carbon film before and after plasma ashing treatment. Here all the spectra have been vertically normalized according to their ZLP heights (ZLP not shown in the plot). The peaks next to ZLP are plasmon peaks. Plasmons are collective oscillations of specimen valence electrons, and their energy loss is usually in the range 10–40 eV. When the TEM sample thickness is thin, for example, less than 30 nm, we can assume the only significant scatter event is a single plasmon event. Thus, the formula above can be modified into a simpler expression:

$$t = \lambda_p \times (I_P / I_0) \quad (2)$$

where λ_p is the characteristic plasmon mean free path, and I_p is the integrated intensity of plasmon peak in the EELS spectrum.

According to this new formula, the intensity change of plasmon peak can directly reflect the thickness change for each spectrum as we normalize ZLP for all the spectra in the Figure 4a. Thus we can say the holey carbon film becomes thinner after downstream plasma ashing treatment by just looking at the decreasing plasmon peak intensity. More quantitatively, we have adopted the log-ratio technique, which is embedded in the Gatan DigitalMicrograph (DM) program and is based on Equation 1, to calculate the thickness of the holey carbon film. Figure 4b shows the calculated thickness change of holey carbon film plotted as a function of downstream plasma ashing time. This shows that the holey carbon film thickness decreases with the increasing downstream plasma ashing time. The data points are collected from the film area in the same grid opening. The as-received holey carbon film thickness is calculated to be 27 nm ± 3 nm, which is consistent

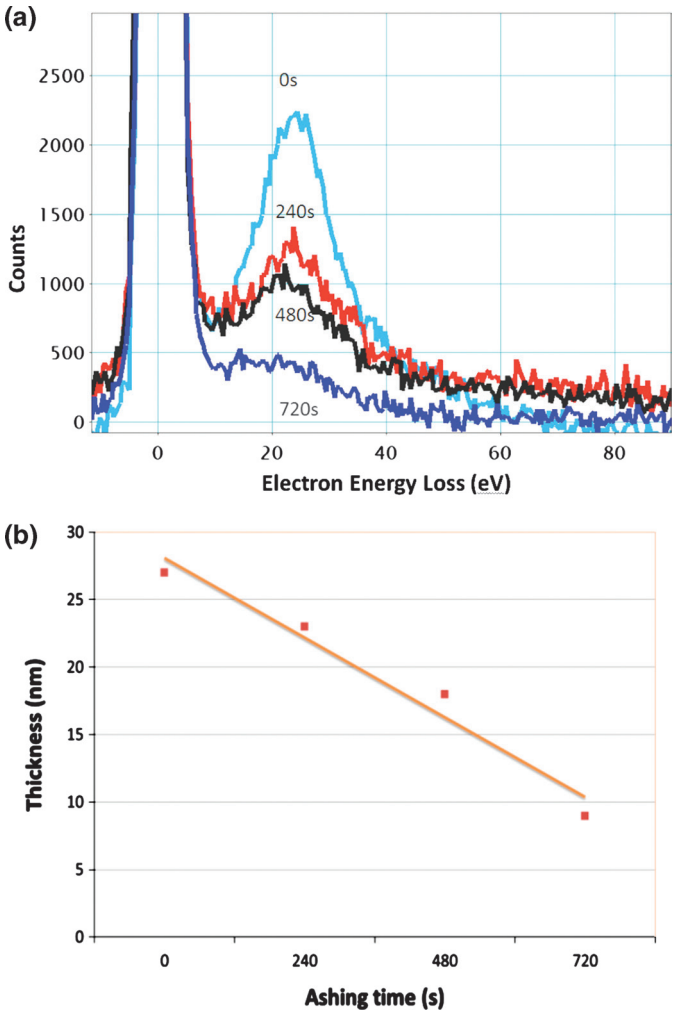

Figure 4: (a) Low-loss EELS of holey carbon support film before and after downstream plasma ashing treatment. (b) Thickness of holey carbon support film as a function of downstream plasma ashing time.

with what the grid supplier claims. The last data point is collected after the film is downstream plasma-ashed for 720 s. At this condition, the carbon film is close to break-up; therefore, the thickness measurement is ambiguous because some film areas are already ruptured. Luckily, the film area we selected for data collection was still intact. The holey carbon thickness we measured for the 720 s ashing was 9 nm ± 3 nm. At such a thin thickness, the holey carbon film is very fragile and probably at a critical point. Thus, any internal stress or even an air pressure fluctuation during sample loading and unloading could be sufficient to rupture the film. Based on these data points, we calculate the etching rate of holey carbon film during downstream plasma ashing treatment as about 1.5 nm/min. This can be a good reference for our routine downstream plasma ashing procedure. Once we have the film thickness value for any as-received holey carbon film, we may estimate the safe ashing time window based on the etching rate.

Specimen cleaning efficiency. Next, it is necessary to evaluate if the GV10x DS Asher can effectively clean the hydrocarbon contamination on the TEM sample. Figure 5a shows the STEM image from a typically contaminated sample loaded on a holey carbon support film Cu-grid. It shows signs of significant contamination under the electron beam as marked by an arrow. The contamination mark grew quickly after electron beam was placed on the region of interest. After only a 60 s exposure, nearly half of the field of view was covered by the contamination mark, and its size extended up to 300 nm. In order to understand the source of the contamination, we used EDX microanalysis to analyze the contamination mark. A typical EDX spectrum of the contamination mark is shown as unfilled purple in Figure 5b. As determined from the spectrum, there are significant X-ray signals from foreign elements Si, C, and O, besides the as-designed shield materials Ni_xFe_{1-x}, detected on the contamination mark. The C and O contamination species are understandable because oxygen

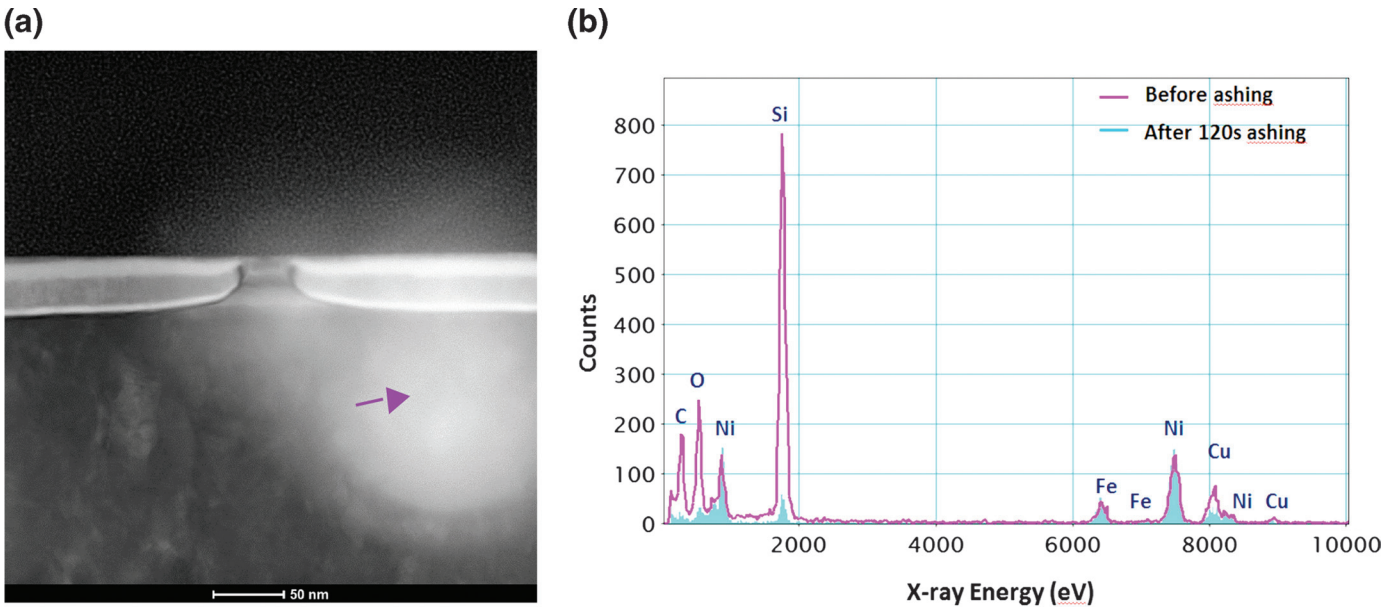

Figure 5: (a) Typical STEM image of a heavily contaminated sample showing the deteriorative effect of carbonaceous contamination build-up. (b) Comparison of EDX spectra on the NiFe magnetic shield material before and after 120 s downstream plasma ashing. Note that each spectrum is acquired from a fresh area.

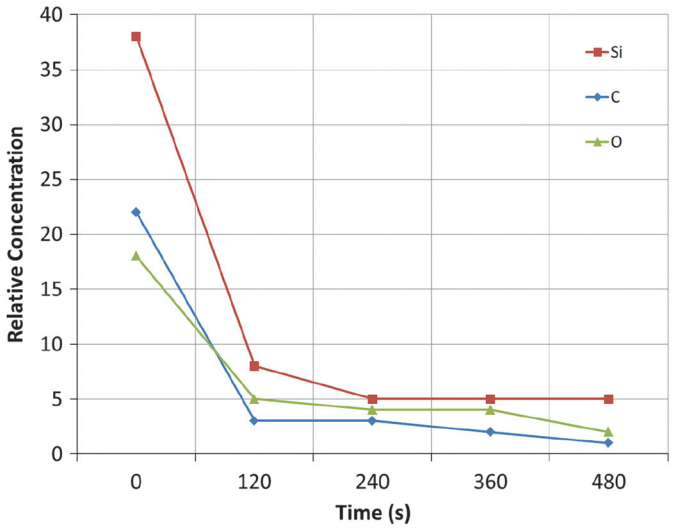

Figure 6: Plots of the contamination species (Si, C, O) as a function of time before and after downstream plasma ashing treatment.

atoms could cross-link with carbon species and form carbon monoxide and a hydrocarbon layer on the sample surface [7]. However, the strong signal of Si was not expected. We confirmed it by multiple analyses.

As far as the experiment goes, we would like to know if the plasma asher system can effectively clean all the contamination species. Because the TEM sample is loaded on a holey carbon support film, we may use the previously determined safe time window as a guide to design the experiment for the downstream plasma ashing experiment. We decided to use 120 s as an interval to test downstream plasma ashing clean efficiency. The filled blue plot in Figure 5b is the EDX spectrum from a fresh area after the sample was downstream plasma-ashed for 120 s. We see from this comparison that the contamination species C and O were significantly decreased compared to the pre-treatment. The unexpected contamination species Si peak is also greatly reduced from 800 counts to 50 counts.

Figure 6 shows that all the three contamination species decease drastically after the sample was ashed for 120 s. Longer clean times could further reduce the concentration of contamination species but not as obviously as in the first 120 s.

Discussion

The effective ashing time of 120 s is much shorter than the time of 720 s for breakup of the holey carbon support film. This means that the TEM sample on the holey carbon support film is safe to be cleaned in such a downstream asher system. More importantly, the sample can be cleaned multiple times. This is useful for the case when the treated TEM samples are stored over a long time and the sample contamination appears again.

Conclusion

Plasma cleaning has become an essential step in modern analytical electron microscopy, which requires contamination-free samples for imaging and elemental analysis. However, the dilemma for carbon film TEM grid users is how to plasma-clean the hydrocarbon contamination while preserving the carbon support film. In order to solve this problem, we have evaluated a new downstream plasma asher system, which uses a gentle and non-kinetic clean mechanism to minimize the side effects of plasma-sample interactions. The results show the system can effectively remove the contamination while preserving the carbon support film. A safe time window and a rule-of-thumb cleaning recipe for this system are suggested.

References

[1] LF Fu, SJ Welz, ND Browning, M Kurasawa, and PC McIntyre, *Appl Phys Lett* 87(26) (2005) 262904–06.
[2] JT Grant, SD Walck, FJ Scheltens, and AA Voevodin, *Mat Res Soc Symp Proc* 480 (1997) 49–71.
[3] C Soong, P Woo, and D Hoyle, *Microscopy Today* 20(6) (2012) 44–48.
[4] TC Isabell, PE Fischione, C O'Keefe, MU Guruz, and VP Dravid, *Microsc Microanal* 5 (1999) 126–35.
[5] SP Roberts, NJ Zaluzec, SD Walck, and JT Grant, *Mat Res Soc Symp Proc* 480 (1997) 127–36.
[6] H Wang, J Fang, J Arjavac, and R Kellner, *Microscopy Today* 16(1) (2008) 24–27.
[7] HG Tompkins and JA Sellers, *J Vac Sci Technol A* 12(4) (1994) 2446–50.
[8] GJ Gorin, *U.S. Patents* US6263831B1, 2001, US6112696A, 2000, US7015415B2, 2006.
[9] DB Williams and CB Carter, *Transmission Electron Microscopy: A Textbook for Materials Science*, Springer, New York, 2009.

MT